Environmental Science and Pollution Research (2021) 28:32609–32625
https://doi.org/10.1007/s11356-021-12989-5

RESEARCH ARTICLE

Variations and similarities in structural, chemical, and elemental properties on the ashes derived from the coal due to their combustion in open and controlled manner

Virendra Kumar Yadav[1] · Govindhan Gnanamoorthy[2] · Marina M. S. Cabral-Pinto[3] · Javed Alam[4] · Maqusood Ahamed[4] · Neha Gupta[5] · Bijendra Singh[6] · Nisha Choudhary[7] · Gajendra Kumar Inwati[8] · Krishna Kumar Yadav[5]

Received: 12 November 2020 / Accepted: 11 February 2021 / Published online: 24 February 2021

Abstract

Coal fly ash (CFA) and coal-based incense sticks ash (ISA) have several similarities and differences due to the presence of coal as a common component in both of them. CFA are produced from the combustion of pulverized coal during electricity production in the thermal power plants while ISA are produced from the burning of incense sticks at religious places and at houses. A typical black colored Indian, incense sticks are mainly are comprised of coal powder or potassium nitrate, wood chip, fragrance, binder or binding agent, and bamboo sticks. The black colored incense sticks have coal powder or charcoal as a facilitator for smoother burning of incense sticks. The detailed investigation of CFA and ISA by X-ray fluorescence spectroscopy (XRF), electron diffraction spectroscopy (EDS), inductively coupled plasma-atomic emission spectroscopy (ICP-AES), Fourier transform-infrared (FTIR), X-ray diffraction (XRD), particle size analyzer (PSA), field emission scanning electron microscopy (FESEM), and transmission electron microscopy (TEM) revealed the morphological, chemical, and elemental properties. Both the coal based ashes comprises minerals like calcites, silicates, ferrous, alumina, and traces of Mg, Na, K, P, Ti, and numerous toxic heavy metals as confirmed by the XRF, ICP-AES, and EDS. While, microscopy revealed the presence of well-organized spherical shaped particles, namely cenospheres, plerospheres, and ferrospheres of size varying from 0.02 μm to 7 microns in CFA. Whereas, ISA particles are irregular, aggregated, calcium to carbon rich whose size varies from 60 nm to 9 microns and absence of well-organized spherical structures. The well developed and crystalline structure in CFA is due to the controlled combustion parameter in thermal power plants during the burning of coal while incense sticks (IS) burning is under uncontrolled manner. So, FTIR and XRD confirmed that the major portion of fly ash constitutes crystalline minerals whereas ISA have mainly amorphous phase minerals. CFA have ferrospheres of both rough and smooth surfaced, which was absent from the ISA and hence ferrous particles of CFA are of high magnetic strength. The detailed investigation of ashes will lead to the applications of ashes in new fields, which will minimize the solid waste pollution in the environment.

Keywords Fly ash · Incense sticks · Incense sticks ash · Ferro-aluminosilicates · Unburned carbon · Soots

Responsible Editor: Philippe Garrigues

✉ Krishna Kumar Yadav
envirokrishna@gmail.com

[1] School of Lifesciences, Jaipur National University, Jaipur, Rajasthan 302017, India

[2] Department of Inorganic Chemistry, University of Madras, Guindy Campus, Chennai, Tamil Nadu 600025, India

[3] Department of Geosciences, Geobiotec Research Centre, University of Aveiro, 3810-193 Aveiro, Portugal

[4] King Abdullah Institute for Nanotechnology, King Saud University, P.O. Box-2455, Riyadh 11451, Saudi Arabia

[5] Institute of Environment and Development Studies, Bundelkhand University, Kanpur Road, Jhansi 284128, India

[6] School of Chemical Sciences, Central University of Gujarat, Gandhinagar, Gujarat, India

[7] School of Nanosciences, Central University of Gujarat, Gandhinagar, Gujarat 382030, India

[8] Department of Chemistry, Kadi Sarva Vidayalya, Kalol, Gandhinagar, Gujarat, India

Introduction

Every year, a million tons of coal are extracted from mines in India which are mainly used for the generation of electricity by the coal-based thermal power plants (CTPPs) (Malav et al. 2020; Yadav and Fulekar 2020) while remaining is used as a fuel, and in preparation of coal-derived material, for instance, incense sticks paste (Ogunsona et al. 2020; Yadav et al. 2020a, 2020b). Due to such a huge amount of burning of coal in thermal power plants (TPPs), annually, there is a generation of million tonnes (MTs) of coal fly ash (CFA) (Kanchan et al. 2015). In the first half of the current year 2019–2020, about 406.91 MTs coal was used by the TPPs, which produced 129.09 MTs of fly ash, out of which 100.94 MTs (78.19%) was consumed while remaining 28.15 MTs was unused which was dumped off in the near vicinity of the TPPs (CEA 2019). The utilization of fly ash includes making of fly ash based tiles, ceramics, bricks, panels, and in metallurgy (Cabral-Pinto et al. 2020; Yadav and Pandita 2019; Sharma et al. 2015; Tavker et al. 2021). CFA are used in civil engineering like dams construction, pavement blocks, road embankments, fly ash construction, fly ash amended cements, land-fills, bricks, and ceramic tiles. Nowadays, fly ash is used for the manufacturing of kitchen panels as a substitute for granite panels (Sharma et al. 2016; Golden Makaka 2014). Fly ash are also used an economical adsorbents, for the wastewater treatment (Yadav and Pandita 2019; Gupta et al. 2015). Fly ash is also used in the manufacturing of geopolymers (Zhuang et al. 2016) or zeolites (Gerardo et al. 2020) which finds application in the research and industries. Besides these, fly ash are also used in the recovery of value added minerals, elements in metallurgy, their separate structural components in paints (Cabral-Pinto et al. 2014; Satapathy et al. 2010) and thickening agent (Miricioiu and Niculescu 2020). While, coal also finds application in the preparation of incense sticks paste for the manufacturing of incense sticks or agarbatti (Yadav et al. 2020b). The coal powder is mixed with, sawdust, Jigat and fragrances where the role of coal powder is to facilitate the smoother burning of incense sticks (Qin et al. 2019; Alam et al. 2017).

India is one of the largest producer, exporter and consumer of incense sticks in the whole world due to high demand of incense sticks and availability of raw materials and labor (Yadav et al. 2020c). In India, being a religious country, there is a common practice of burning of incense sticks at most of the religious places especially temples, mosques, and most of the houses (Dewangan et al. 2013). Consequently, every year, a million tonnes (MTs) of coal powder-based (which are generally black in color due to coal or charcoal) incense sticks are lighted (Yadav et al. 2020c) that leaves behind a gray to an earthen color residual product called incense sticks ash. Moreover, in Hinduism ISA is considered sacred due to which in a country like India, is always disposed of only in the river and other water bodies. This situation gets more aggravated as India is considered a land of religious places where every day tons of ISA are produced and disposed of into the water bodies. So, dumping of ISA into the river leads to water pollution, by increasing the heavy metal content, water hardness and alkalinity (Gupta et al. 2021; Yang et al. 2006). Indian incense sticks manufactures uses calcium phthalate to minimize the smoke in the incense sticks; consequently, ISA have comparatively higher calcium content than ISA of other countries (Lin et al. 2008; Yadav et al. 2020a). Besides, this Indian ISA also have a high amount of Mg, Na, and K alkali metals (Yadav et al. 2020a, 2020c) due to the use of potassium nitrate as a burning agent in white or colored incense sticks. As black colored incense sticks use coal or charcoal powder which have high ferrous, alumina, and silica content along with numerous toxic heavy metals, so, all these elements are also present in the Indian ISA.

As, both CFA and incense sticks use coal or coal powder directly or indirectly (Lin et al. 2008, a) so it is assumed that both the ashes have various similarities and differences between them. But as ISA has few other ingredients also so, the composition of both CFA and ISA varies from each other (Thipse et al. 2002; Abdelrazek et al. 2018). As coal is formed from organic material so, it has numerous organic compounds that burn in the thermal power plants during burning of coal (Aich et al. 2019). The ferrous, silica, and alumina are present in CFA in the form of ferro-aluminosilicate (Miricioiu and Niculescu 2020), which is also expected in the ISA but the concentration should be low. Both the ashes have numerous amorphous and crystalline phase minerals or materials which form during combustion (Yadav et al. 2020b) but the coal in TPPs burns under controlled parameters whereas incense sticks burn under uncontrolled conditions.

From the previously reported work, it is well known that CFA is micron-sized, spherical shaped materials having structurally variable particles like cenospheres (Manocha et al. 2011; Ranjbar and Kuenzel 2017), precipitators (Sear 2001), plerospheres (Haustein and Kuryłowicz-Cudowska 2020), ferrospheres (Liu et al. 2020; Choudhary et al. 2020; Menazea 2020), and carbon particles including both unburned and soots (Salah et al. 2016). CFA particles are the assembled products formed by the combustion, melting, and solidification of mineral components (Assi et al. 2020). Cenospheres and plerospheres normally dominate the morphology in finer fractions of CFA while larger particles may be irregular which has variable amounts of bubbles and higher contents of crystalline minerals (Wrona et al. 2020). Based on minerals, CFA has both inorganic and organic phases (Fuller et al. 2018). Among inorganic phases (crystalline and non-crystalline), three major crystalline phases are quartz, mullite, and spinels, and non-crystalline or amorphous aluminosilicates glass (Prochon et al. 2020). The major minerals in CFA consist of mullite ($3Al_2O_3{\cdot}2SiO_2$), quartz (SiO_2), aluminum oxide

(Al_2O_3), hematite (Fe_2O_3), lime (CaO), gypsum, and rutile (TiO_2) (Liao and Guo 2019). There are variations in the physical, chemical, and mineralogical properties of CFA depending on the mineral composition of used coal and combustion technology (Choo et al. 2020).

While on the other hand, the major fractions of incense sticks are composed of organic matter which gets volatilized during the combustion of incense sticks (Yadav et al. 2020b). The complete combustion of incense sticks produces ash up to one-tenth of the actual weight of incense sticks. Until now, very limited information is available in the scientific community about incense sticks ash production, utilization, chemical composition, and application. Indian incense sticks manufacturers use around 15–25% by weight charcoal or coal powder as an additive to the incense sticks paste to facilitate the smoother burning of incense sticks (Yadav et al. 2020a). So, the composition of ISA is expected up to 25–50% similar to those of CFA. But the structural components could vary as combustion of coal is carried out in a controlled system in the TPPs (Marjanović et al. 2020) while the burning of incense sticks is carried out in an uncontrolled manner (Wang et al. 2006; Yadav et al. 2020b). So, there is a possibility in the variation of oxygen, temperature, and other environmental factors in the combustion of coal and incense sticks. The combustion of coal in TPPs is relatively carried out at very high temperature, i.e., 900–1800 °C (Bartoňová 2015), whereas the combustion temperature of incense sticks is below 150 °C. Moreover, ISA may also have high unburned carbon contents due to incomplete burning at lower temperatures. Secondly, it could also be due to the organic content in the form of fragrance and bamboo sticks used. So, in order to know the detailed information about the ISA their similarities and differences with the CFA and their parent material, i.e., coal, it is important to thoroughly characterize both CFA and ISA reveal the complete chemical composition, mineralogical and morphological properties of the incense sticks ash.

The novelty of the present research works lies in the fact that, here we have first time the comparative and descriptive morphological and elemental analysis of fly ash and incense sticks ash. The study will help in opening new horizons in their recent and emerging applications especially for recovery of value added minerals. Moreover, the current research works, emphasizes the prerequisite conditions for obtaining industrially important ISA and CFA.

The major objective of the current research work is to find out the major similarities and differences between the two types of ashes derived from coal. Another objective of this current research work is to represent ISA as economical and potential waste for the recovery of value added minerals like carbon particles, ferrous, silica, alumina and calcium and magnesium oxides. Another, objective of this work is to suggest a safe and effective method for the disposal of ISA. One final objective of the current research work is to find out the various factors which are responsible for providing well developed ceramic properties to CFA and irregular and unorganized structure to ISA.

In the present research work, CFA was collected from Gandhinagar TPPs, Gujarat, and ISA was collected from the local temples in Gandhinagar, Gujarat, India. Both CFA and ISA were comprehensively characterized by X-ray fluorescence spectroscopy (XRF), electron diffraction spectroscopy (EDS), inductively coupled plasma-atomic emission spectroscopy (ICP-AES), Fourier transform infrared spectroscopy (FTIR), X-ray diffraction (XRD), particle size analyzer (PSA), field emission scanning electron microscopy (FESEM), and transmission electron microscopy (TEM) for the detailed morphological, chemical and elemental properties. The present study will help in deciding the application of these two by-products, either in the manufacturing of composite materials from them or in materials like geopolymer or zeolites. The geopolymer binders can be used as concrete, masonry units, and concrete material (Ahmari and Zhang 2015). Moreover, the study will also help in determining their possible future applications in addition to safe handling and disposal.

Materials and methods

Sample collection

The CFA sample was collected from Gandhinagar thermal power plant where the CFA was directly collected from the electrostatic precipitator in the sterilized plastic silos. Incense sticks ash (ISA) was collected in a sufficient amount for 4–5 days regularly from a temple situated Gandhinagar, Gujarat, India.

Materials

Fly ash, incense sticks ash, sieve sets, beakers

Preparation of ISA and CFA

After bringing the ISA into the laboratory, it was sieved to eliminate the larger particles, incompletely burned materials, and bamboo sticks. Further, it was dried in an oven at 105 °C, overnight to remove any moisture. Then the fine incense sticks ash was analyzed by a series of characterization techniques for the detailed elemental, morphological and mineralogical properties of incense sticks ash. The CFA samples were dried in an oven in the laboratory at 105 °C for 24 h before analysis. Figure 1 shows the physiological appearance of coal fly ash and incense stick ash.

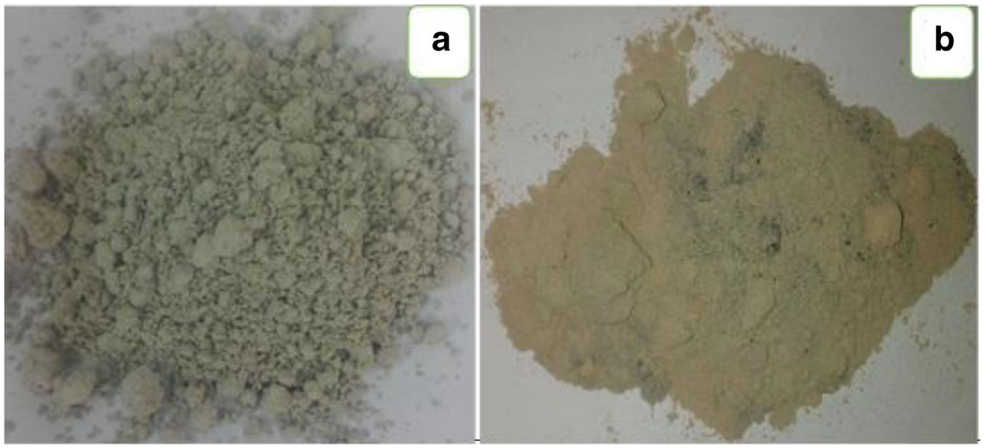

Fig. 1 Images of coal fly ash (**a**) and incense stick ash (**b**)

Characterization of CFA and ISA

The physicochemical analysis (pH, color, carbon content) of both CFA and ISA was done. Inductively coupled plasma-atomic emission spectroscopy (ICP-AES) helps in the detection of trace elements in CFA in the form of the liquid samples. The total element detection in both ashes was done by ICP-AES in a liquid form. The samples for ICP-AES were prepared by treating both the samples by aqua-regia and digested on a hot plate at 180 °C until complete dryness. About 0.5 g of CFA and ISA was taken in two separate 50 ml Teflon coated crucible into which initially 10 ml of hydrofluoric acid (HF) was added and heated until dryness, which was followed by addition of 10 ml conc. H_2SO_4, 10 ml conc. HNO_3 and finally 25 ml of conc. HCl. The sample was filtered and the analysis was done by SPECTRO ARCOS, Analytical instruments GmbH, Germany simultaneous ICP Spectrometer. The X-Ray Florescence spectroscopy analysis helps in the detection of major elemental oxides and chemical composition of both CFA and ISA. The analysis was carried out by using Horiba, Japan makes and model no. XGT-2700 X-ray analytical microscope fitted with High purity silicon detector (XEROPHY) X-ray tube with Rh target. For XRF analysis, about 5–8 g of CFA and ISA were mixed thoroughly with the barium chloride, separately and a pellet was prepared for the identification of major elemental oxides.

The FTIR analysis was done for detecting various functional groups, and microcrystalline structures present in the samples. FTIR analysis was carried out by a solid pellet method, where the CFA and ISA samples were mixed separately with KBr powder in the ratio of 2:98. The thoroughly mixed samples were then pressed by a mechanical press machine to obtain a pellet. Further, the FTIR measurements of both the samples were done in the range of 400–4000 cm^{-1} by using a Perkin-Elmer spectrum 6500 instrument at a resolution of 2 cm^{-1}. XRD was done for the phase identification of various amorphous and crystalline minerals present in the CFA and ISA. The XRD patterns were recorded using a PHILIPS X'PERT PRO instrument equipped X'celerometer. The XRD patterns were recorded in the 2θ range of 20–70° with a step size of 0.02 and a time of 5 seconds per step at 40 kV voltage and a current of 30 mA. The particle size analyzer is based on a laser scattering technique that provides average particle size or hydrodynamic size, particle size distribution, and poly dispersity index (PDI).

For particle size analysis (PSA), a pinch of both the samples was taken in a tube to which double distilled water was added. Further, both the samples were sonicated in an ultrasonicator (Sonar 40 kHz) for 10 min. The dispersed samples were used for the PSA measurement at room temperature by using a Malvern Zetasizer S90 (UK). Field Emission Scanning Electron Microscopy was carried out to reveal the surface morphology of the CFA and ISA. Moreover it was also used to differentiate structurally, different types of particles in both the ashes. The analysis was carried out by Carl Zeiss (NOVA, NANOSEM) FESEM, at variable magnification. The analysis was carried out on by spreading ISA on double-sided carbon tape and gold sputtering was done for 10 min. The elemental composition of ISA particles was investigated by the attached Bruker made EDS analyzer. Transmission Electron Microscopy (TEM) helped in the determination of the size and shape of various particles present in both the samples. The shape and size analysis of CFA and ISA particles was done on TECHNAI G2 F20 S-TWIN instruments operated at a voltage of 200 kV. For TEM and HR-TEM measurements, the samples were prepared by drop-casting the particles suspended in aqueous medium on carbon-coated copper grids. The scattering area electron diffraction (SAED) pattern was also analyzed on the same grids.

Results and discussion

Both CFA and ISA are direct and indirect by-products of coal. Coal has high organic content along with Si, Al, Fe, S, C, and O as major elements. Most of the organic minerals present in

the coal and coal powder get transformed into their respective inorganic form during the combustion of coal (Ward 2002), and incense sticks. So, it is expected to have Si, Al, Fe, C, S, and O as major elements in both the types of ashes.

The color of CFA varies from grayish black to white which depends on mainly carbon content and on CaO content. The higher the carbon content in the CFA the darker will be its color, while the higher the calcium oxide (CaO) content then the shade will be white. While, the color of ISA is mainly gray to tan color due to the high amount of carbon content (Yadav et al. 2020b). Moreover, Indian ISA has 50% calcium oxides due to which it is mostly in white shade.

The texture of CFA particles is smooth and consistent because the burning of coal in thermal power plant is carried out under controlled conditions, where the molten minerals from coal gets sufficient time for cooling of the particle and attain specific shape, and nature. Whereas, the consistency of ISA particles is not like CFA, as it is not fine powder, rather some particles are in coarse size, some in fine size while few will be large unburned incense sticks particles or residue of bamboo sticks.

The pH of CFA varies from 7 to 9 depending on the presence of alkaline materials in coal (Palomo et al. 2014). Alkalinity and high pH of CFA are due to the presence of CaO, Na_2O, and other alkali metals (Fernández-Jiménez et al. 2014). Wilińska and Pacewska (2019) reported that the pH of CFA varies from acidic to alkaline based on the content but it is mainly alkaline due to the presence of alkali metals that form hydroxides. Similarly, the pH of ISA is also ranges between 7 and 9, i.e., alkaline in nature. The alkaline nature of ISA might be due to the increased formation of calcium hydroxides ($Ca(OH)_2$), magnesium hydroxides ($Mg(OH)_2$), and sodium hydroxides (NaOH). The increased formation of $Ca(OH)_2$, $Mg(OH)_2$, and NaOH was due to the high concentration of Ca, Mg, and Na in ISA (Table 1) because these metals form their respective hydroxides when get in contact with water. Traditionally, a typical composition of incense sticks consists of 21% (by weight) of herbal and wood powder, 35% of fragrance material, 11% of adhesive powder, and 33% of the bamboo stick (Lin et al. 2008).

ICP-AES for detection of chemical elements

As the CFA is has a very harsh structure in which most of the elements are present in complex bonds in the crystalline form so the hydrofluoric acid leaches out firmly bound inert elements from the CFA particles. The qualitative analysis of CFA indicated the presence of Ag, Al, As, B, Ba, Ca, Ce, Cl, Co, Cr, Cu, Dy, Be, Eu, Fe, Ga, K, La, Li, Lu, Mg, Mn, Mo, Na, Nb, Ni, P, Pb, S, Sc, Si, Sm, Sr, Th, Ti, V, Y, Yb, Zn, and Zr (C, H, N, O, Hg, Cd). While the quantitative analysis of the CFA sample revealed that most abundant element present in CFA sample were silica, alumina, and iron along with C, Cl, K, Na and S. It was noted that most of these major constituents are volatile elements, which were formed due to the high temperature and excellent burnout during the incineration process (Leelarungroj et al. 2018). The minor elements were mainly heavy metals like Pb, Ti, and Zn. The other elements present in very trace quantity were Ba, Cd, Co, Cr, Cu, Mn, Ni, and Sr. Beside this, the CFA has several rare-earth elements like Y (yttrium), Dy (dysposium), Yb, V, Er (erbium), Ce (cerium), Sc (scandium), Sm, and Lu. Besides this, it also has radioactive elements like thorium (Th). Besides this, it has several toxic heavy metals like Ni, Zn, Pb, Cd, Cr, Co, Mn, Mo, and Co. It has alkaline earth metals (Be, Sr, Ba, Mg), alkali metals (Li, Na, and K), and metalloids (B and Si).

Table 1 Concentration of elements present in CFA and ISA detected by ICP-AES

Elements	CFA (mg/ml)	ISA (mg/ml)
Al	125.5	-
Fe	123.0	378
Mg	41.9	-
Mn	97.1	24.98
Cd	80.2	0.002
Co	96.9	0.305
Cr	95.3	1.771
Cu	88.6	3.602
Ni	95.2	1.284
Pb	0.9	0.156
Zn	109.0	2.825
Ca	-	195.8
Mo	-	0.056
Se	-	0.014
Sr	-	5.327
Ti	-	0.120
Li	-	0.259
Sb	-	0.164
V	-	0.378
As	1132.5 μg/l	-

ISA also has most of the elements present in the CFA sample, except As and Hg, while Al and Mg were not detected in the samples. The ISA consists heavy metals, like Cu, Co, Sr, Cr, Pb, Cd, Ni, Zn, and Mo (Verma et al. 2014). Among all the heavy metals, Mn was present in the highest concentration and Cd was present in the least concentration in the ISA liquid sample. The dumping of such ashes onto the land or in the water bodies may pose a potential threat for the vegetation and aquatic organisms due to the leaching of toxic heavy metals into the soil and water. However, the leaching of heavy metals depends on the pH of the soil and water. The lower pH and acidic conditions favors the leaching of most of the metals

from CFA and ISA while the higher pH or alkaline conditions slows down the leaching of heavy metals (Prasad and Mondal 2008; Leelarungroj et al. 2018). Table 1 shows the concentration of elements present in ISA and CFA.

XRF: major oxides in CFA and ISA

XRF is a fast, economical, reliable non-destructive method for the quantitative analysis of elements from Fluorine to Uranium in their oxides forms (Misra and Mudher 2002). The composition of major elements in the oxides form of CFA and ISA are given in Table 2. The major elemental oxides of CFA as given in Table 2 is silica (SiO_2), alumina (Al_2O_3), ferrous (Fe_2O_3), sodium dioxide (Na_2O), and titanium dioxide (TiO_2) which alone comprises 96.6% and the remaining 3.4% is constituted by oxides of Ca, Mg, Na, K and P. The silica content is 56.98%, alumina 27.07%, and ferrous oxides is 5.4%, so the total ferro aluminosilicates content is 89.4% in the CFA. Even if CaO will also be included then this value will reach 90.4%. Besides this CFA also have CuO (0.2%) and SrO (0.02%) as toxic heavy metal oxides. While the major elemental oxide of ISA is calcium oxides, silica, alumina, ferrous, potassium oxide, phosphorus oxide, and magnesium oxide; all these major elemental oxides constitute about 95.11% while the remaining 4.89% is constituted by oxides of trace elements. The total FAS content in ISA is about 29.41% while on the inclusion of CaO this value reached 79.63% for Ca + FAS. The ISA is a complex mixture of Ca, Si, Al, Fe, C and Mg having a heterogeneous distribution of elements on the surface. Besides this, ISA also has Na, K, Mg, Ti, Ni, Cu, Sr, P, and S in the form of oxides in a small amount. Besides this, ISA also has toxic heavy metal oxide, i.e., CuO (0.87%), and SrO (0.12%). It has numerous toxic heavy metals also, in small quantity so, it was not detected by the XRF as it can detect only major element oxides.

Table 2 Elemental composition of CFA and ISA by XRF

Elements	CFA (%)	ISA (%)
SiO_2	56.98	20.36
Al_2O_3	27.07	4.77
Fe_2O_3	5.40	4.28
MgO	0.00	3.91
P_2O_5	1.95	3.94
CaO	1.096	49.61
K_2O	1.16	8.24
TiO_2	2.90	0.60
Na_2O	4.25	0.97
MnO_2	0.06	0.15
SO_3	0.04	3.77
CuO	0.20	0.87
SrO	0.02	0.12
Total	100.67	99.99
Si/Al Ratio	2.10	4.26
F + A + S	89.45	29.41
Ca + F + A + S	90.54	79.02

The XRF analysis of both CFA and ISA revealed that though both ashes have been derived from coal, as the CFA is directly derived from coal so, there is a high content of FAS in CFA, i.e., 89.4% while in ISA it was 29.41% only as in incense sticks paste a small fraction of coal powder is added (Ramya et al. 2013). So, the FAS content in CFA was almost three folds than the ISA because their parent coal has majorly these three elements only along with sulfur (Yadav and Fulekar 2020). While in incense sticks as only a small amount of coal powder is used so the FAS content is low. While based on the source of coal, fly ash could be class F and class C, where class F is derived from anthracite and bituminous source of coal, and total FAS content is more than 75% and CaO is less than 5%. So, the CFA belongs to class F (Yadav and Pandita 2019), whereas Indian incense sticks use Ca phthalate so, there is high CaO content in ISA; While the potassium oxide content is very high in the ISA in comparison to the CFA.

The major differences between the elemental compositions of CFA and ISA might be due to the fact that CFA comes from clay and quartz in the coal, and iron-bearing mineral-like pyrite in the coal provides Fe_2O_3 content in CFA. The source of the CaO and SO_3 in CFA is calcium, mostly from calcium carbonates and calcium sulfate in the coal. Such types of low-lime CFA are the typical characteristic feature of Indian fly ashes that have higher alumina, silica and lower ferrous content (Ayanda et al. 2012). This indicates the higher fusion temperature and consequently lower chances of formation of glass.

The CFA reactivity depends on the glass content and other minerals phases present in it (Jóźwiak-Niedźwiedzka et al. 2018). Here the network formers (F + A + S = 87.77%) and network modifiers (Na_2O + K_2O + CaO + MgO = 9.285%) ratio are much higher and imbalanced in the CFA. The ratio of network formers to network modifiers is 9.45, which indicates the lower glass content present in the CFA (Aughenbaugh et al. 2016). While the network formers (F + A + S = 29.41%) and network modifiers (Na_2O + K_2O + CaO + MgO = 62.73%) ratio in ISA is much low which is 0.46% which is much lower the CFA. The ISA has a comparatively higher amount of both the toxic heavy metal oxides, i.e., CuO and SrO. CuO was more than four folds in the ISA than the CFA and SrO was 6-fold in ISA than the CFA. Both the heavy metal oxides were present in higher amounts in ISA than CFA even when only a small fraction of coal powder was used in the incense sticks paste. So, in the ISA the source of both CuO and SrO might be other than coal. Table 2 shows the XRF analysis of the elemental oxides present in CFA and ISA.

EDS analysis for elemental composition of CFA and ISA

The EDS analysis of CFA and ISA reveals the major elements present on their surface. The EDS spectra were obtained by selecting an area on the sample, the beam was focused and elemental data was acquired. Nevertheless, the predominant elements in all the CFA particles are Al, Si, C, O, and C where Al was mainly associated with the silicon (Ohenoja et al. 2020). The compositions of these four elements vary from region to region of CFA particles along with the minor elements but generally, Si-Al is more prevalent on the CFA particles. The carbon indicates the unburnt carbon and soots present in the CFA (Fuller et al. 2018); While Ca, Mg, Na, and Ti are present in the form of oxides along with Al, Si, and Fe with varying composition. The EDS analysis of fly CFA reveals the chemically and elementally heterogeneous nature of the CFA, as the elements are present unevenly on the surface of CFA particles. The EDS of CFA revealed that about 72% of the particle is made up of aluminosilicates. Figure 2a exhibit the EDS spectra of CFA, which clearly show prominent peaks for C, Si, Al, Fe, O, Mn, Mg, Ca, Na, Ti, P, and K. The highest element present was O, Al, Si, and Fe in the CFA while Mg, Ca, and K were present in small amount, i.e., below 1%.

While the EDS spectra of ISA in Fig. 2b show peaks for Ca, O, Si, Al, C, Mg, and K. These elements are present mainly in the form of oxides. Carbon is present in the highest percent, i.e., 31.28% which is due to the bamboo sticks, fragrance material, and sawdust and coal powder. All these are sources of carbon content in the ISA. The higher carbon source is also due to the utilization of wood chips and powder which facilitates the ignition of incense sticks. Carbon is due to incomplete burning, soots, and PAH (polyaromatic hydrocarbons) and PCHs (poly cyclic hydrocarbons) present in the incense sticks. Ca was present in 21% which is due to the use of calcium source in the incense sticks. Silica content is 3.59% followed by traces of K, Mg and Al 1.45, 1.53, and 1.12% respectively. The elemental composition obtained by FESEM-EDS is justified by the XRF data of ISA.

The elemental composition detected by the EDS revealed that both the ashes have almost the same elements, which are given above in the table, except Fe and Ti which was present in CFA and not detected in ISA; though both the elements were detected by the ICP-AES and XRF. This could be because of the reason that the Fe and Ti might be unevenly distributed on the surface of ISA particles.

The major elements in ISA were O, C, and Ca which has a total composition of about 92.82% (wt.); while in CFA, the

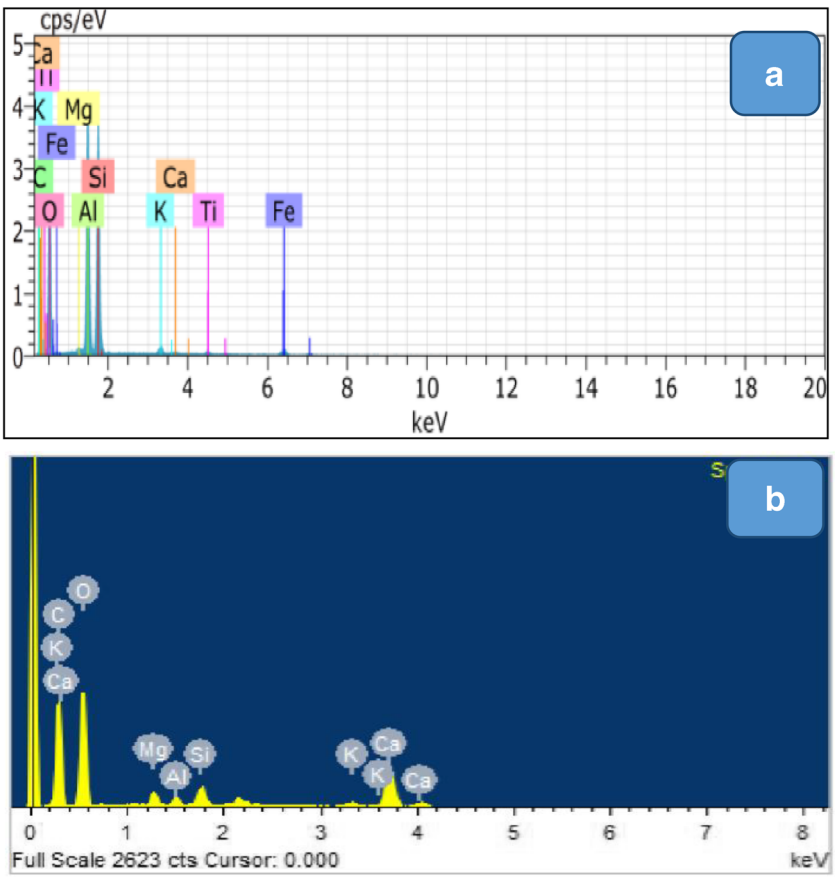

Fig. 2 EDS spectra of CFA and ISA

major elements were O, Al, Si, and Fe. Calcium was present much less amount in the CFA as it belongs to class F CFA (derived from higher grades of coal) moreover incense manufacturers add calcium phthalate to minimize the smoke released by the incense sticks. As the CFA has a complex mixture of FAS, so it was present in a much higher amount in CFA than the ISA. While, Ca content was almost 84 times more in ISA than the CFA, which was due to two reasons: firstly due to the addition of Ca phthalate in the incense sticks paste and secondly here the CFA was class F which have CaO content less than 15%. Table 3 presents the elemental compositions o CFA and ISA based on EDS analysis.

XRD for phase identification

Generally, CFA particles have 60–90% amorphous while remaining are crystalline (Rosas-Casarez et al. 2018; Shi-Chih and Hsiang-Sheng 1993). The various crystalline phases of CFA are mullite with major 2θ peaks at 26.27°, and 41.12° with d-spacing at 3.328 Å and 2.19 Å respectively. Quartz has major 2θ peaks at 26.78°, 50.018°, and 60.86° with d spacing at 3.32 Å, 1.82 Å. and 1.52 Å respectively. While iron oxides like hematite have 2θ peaks at 33.53°, with d-spacing at 2.67 Å, and magnetite has 2θ peaks at 35.49° and 54.15° with d-spacing at 2.52 Å and 1.69 Å respectively (Wrona et al. 2020). A small peak of calcite is also there at 37°, due to the small content of CaO in class F CFA. Besides this, it also has an amorphous glass phase, which is due to the silica, which shows a hump from 2 theta 20° to 30° (Li et al. 2011).

The XRD diffraction pattern of CFA and ISA is shown in Fig. 3b reveals that the CFA is generally a complex material consists of alumina, silica, and iron in the forms of mullite, quartz, magnetite, hematite, calcite, and cristobalite (Cabral-Pinto and Ferreira da Silva 2019; Valeev et al. 2018). Mullite phases are derived from the kaolinite minerals at a temperature above 1000 °C (Suriyanarayanan et al. 2009).

Table 3 Elemental composition of CFA and ISA by EDS

Elements	Weight % (CFA)	Weight% (ISA)
O	34.21	41.33
Al	12.15	1.12
Si	10.82	3.09
C	1.10	31.28
Fe	3.50	-
K	0.73	1.45
Ti	1.02	-
Mg	0.13	1.53
Ca	0.24	20.21
Total	**63.91**	**100.00**

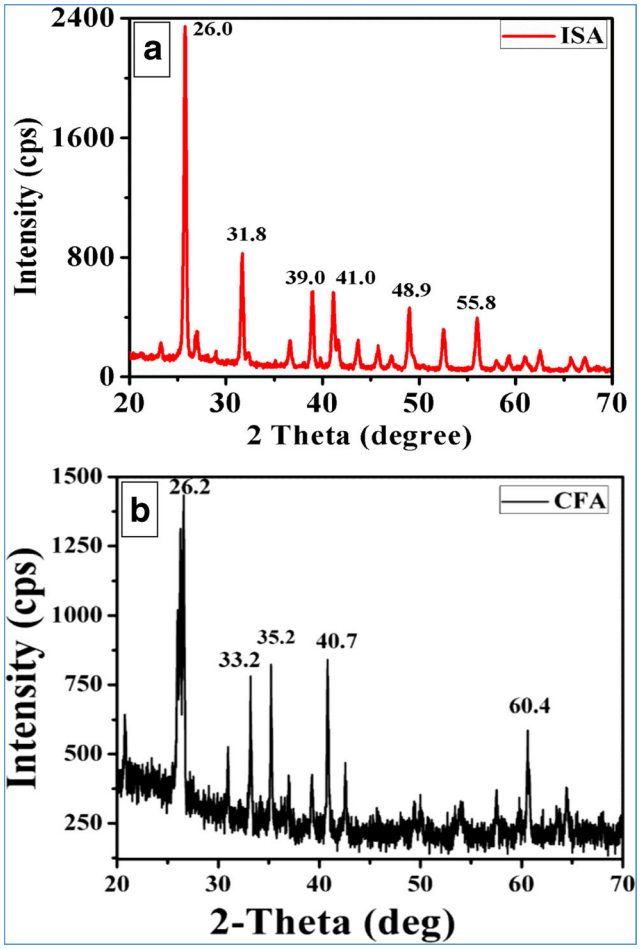

Fig. 3 XRD diffractogram of CFA (**a**) and ISA (**b**)

All these formed during the combustion reaction between the quartz and other minerals phases present in the parent coal. The hematite is formed from the pyrite ores during the combustion of coal at temperature 400–700 °C which is further transformed to magnetite at higher temperature, i.e., 1390 °C. Figure 3b shows a typical XRD pattern of the CFA sample.

While the XRD pattern of ISA in Fig. 3a reveals peaks for the various crystalline and amorphous mineral phases. A small peak at 2θ, 20.82° is due to the carbon or soot particles present in the ISA particles in large content. A small intensity peak at 2θ, 26.68° is due to the quartz (Alehyen et al. 2017) and a small hump at 28.24° is due to the amorphous silica. A very strong and sharp peak at 2θ, 29.40° is due to the crystalline phase of calcium carbonate (Shakkthivel et al. 2005) and several small peaks at 2θ, 35.5, 39.5, 43.1, 47.5, and 48.5°. All these peaks are related to the calcite minerals. The calcite peaks are similar to the work done by (Pal and Gautam 2012). Two small peaks at 2θ, 33.3°, and 36.0° are due to the iron oxide phases, which could be due to the hematite and magnetite phase (Shoumkova 2010; Gomes and François 2000). Both the iron oxides are crystalline in nature.

ISA particles have both amorphous and crystalline phases where amorphous phases are due to silica while crystalline phases are due to the calcite, magnetite, and hematite. From the above analysis, it is found that CFA has major minerals in the form of quartz, mullite, magnetite, and hematite (Vu et al. 2019). While the ISA has calcite, magnetite, and hematite as the major phases where the calcite phase is most prominent with almost 50% which was also supported by the XRF and EDS data.

FTIR for functional group determination

The FTIR is mainly considered for the identification of functional groups present in both the samples. Moreover, it is also used for the determination of the microcrystalline nature of the particles. Here FTIR is used for identification of the bands corresponding to the Si-O-Si/ Al-O-Al, S-O, Fe-O, and C-O bonds in both CFA and ISA (Jeyageetha and Kumar 2013). Figure 4 reveals FTIR spectra of CFA where a broad band around 3400–3000 cm^{-1} are attributed to the surface -OH group of a characteristic of silanol (-Si-OH) and adsorbed water molecule on the surface (Choo et al. 2020; Khatri and Rani 2008). The band around 1635 cm^{-1} is assigned to the bending vibration of –OH groups of water molecules. The range from 1200 cm^{-1} to 500 cm^{-1} represents to quartz and mullite phases of CFA (Mollah et al. 1999). The band at 1088 cm^{-1} is attributed to the v^3 SiO_4 stretching vibrations (Benarchid et al. 2005) in silicates like quartz, cristobalite, and amorphous silica.

The band around 902 cm^{-1} originates from Al-O symmetric stretching vibrations from mullite and band around 562 cm^{-1} is attributed to Al-O-Al/Si bending vibrations (mullite). The band at 455 cm^{-1} is also attributed to O-Si-O/Al-O-Al symmetric bending vibration of quartz and silica (Fernández-Jiménez and Palomo 2005), and in case of tectosilicates like quartz, cristobalite, an additional band is observed at 561 cm^{-1} (Lee and Deventer 2002; Jaarsveld et al. 2003).

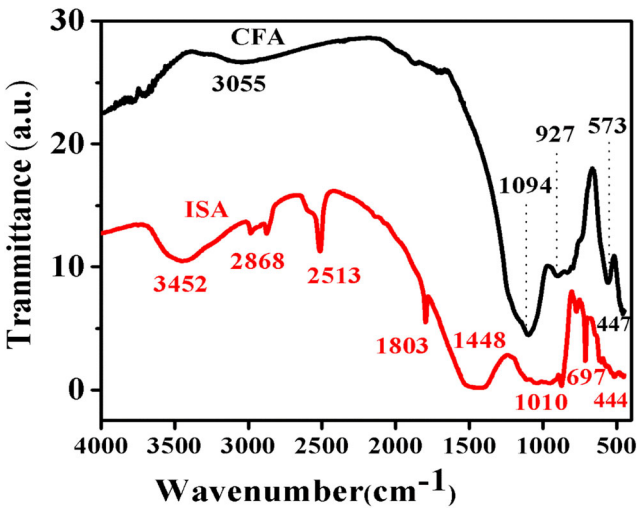

Fig. 4 FTIR spectra of CFA and ISA

FTIR spectra of ISA exhibit a small band at 3452 cm^{-1} which is attributed to the -OH molecule which is either due to adsorption of a water molecule on the surface of the particle or due to the organic molecule in the ISA (Jeyageetha and Kumar 2013). The band at 2863 cm^{-1} is attributed either due to the presence of carbonate group in the ISA. While the band at 2513 cm^{-1} is attributed to the atmospheric carbon adsorbed on the surface of the ISA particles (Bacsik et al. 2004). A strong and sharp band at 1448 cm^{-1} is due to the carbonate group of calcium carbonate (Reig et al. 2002). While the carbonate bands are also at 800 cm^{-1} and 700 cm^{-1} (Shan et al. 2007). The spectrum showed vibrational bands at 1448 cm^{-1}, 876.72 cm^{-1}, 712.72 cm^{-1}, and 409.891 cm^{-1} indicates plane bending vibration of carbonate (Hariharan et al. 2014). A weak band at 1010 cm^{-1} is due to the silicates present in the ISA particles, which are attributed to the Si-O-Si/Si-O-Al (Khale and Chaudhary 2007). These silicates are due to the addition of coal powder in the incense sticks which have a high amount of silicates in them. While the calcium carbonates are due to the addition of calcium derivatives in the incense sticks mixture to reduce the pollution released by the burning of incense sticks. Table 4 gives an account of peaks on the basis of FTIR analysis.

From the FTIR analysis, it was found that both the ashes have silicates, aluminates, and ferrous due to the presence of silicate bond (Si-O-Si), Si-O-Al bond, and Fe-O bonds. While Ca-O and CO_3^{2-} bond was more prominent in the ISA sample which was almost negligible in the CFA (Yadav et al. 2020b). This was because of high amount of either oxides or carbonates of calcium in ISA and lower content of calcium oxide (CaO) in CFA. ISA also has peaks for carbon compounds in the range of 1600–1400 cm^{-1} which was not more prominent in the CFA as it has low carbon content which was also evidenced by XRF and EDS. So, it is confirmed that both the ashes have several groups in common, which might be coming in them from their parent source, i.e., coal.

Particle size analyzer for measurement of particle size distribution

The CFA and ISA particles were firstly dispersed in distilled water under ultra-sonication for 15 min at 15 kHz frequency. The prepared colloidal liquid was then taken for PSA measurements and the graph shown in Fig. 5a, b. For the good result, we have repeated this measurement two times with 1 min/cycle run. The obtained particle distribution along with size, average size, and PDI values are shown in the graph. The CFA particle average size was 788.8 nm, while most of the particles were of size 800.6 nm in diameter with PDI 0.243. While the ISA particle size was 487 nm size and PDI was 0.526 as shown in Fig. 5b. The larger size of the particles

Table 4 Major FTIR assignments of CFA and ISA

0	Nature of bands	CFA	ISA	Minerals
(-Si-)O-H		3055	3452	-
O-H		2323.6		-
Si–O–Si	Asymmetric stretching	1094	1010	-
Si–O–Si	Asymmetric stretching	896.36	906, 832	-
Si-O-Al	Stretching vibration	573	697	Aluminosilicates, mullites
O-Si-O band	Bending vibration	447	444	Quartz

especially may be due to calcium carbonate and ferrous particles were obtained considering its hydrodynamic radius of water molecules as solvent (dispersion medium) and thus large size was observed. The polar molecules of the ISA and water interact onto to the surface obeying electrostatic induced interaction and may be due to that hydrodynamic sphere considered during particle size analysis in PSA. Here, the PDI value indicates the fine distribution of ISA particles in the water solvent as the PDI value is found to be 0.526.

FESEM for surface morphology

FESEM is one of the most reliable and widely used techniques for the morphological features as well as identification and characterization of the various particles present in both CFA and ISA. Figure 6a shows FESEM micrographs of CFA at 200 μm, which shows the spherical shaped particles whose sizes, vary from 0.2 to 7 μ. While Fig. 6b shows spherical CFA particles at 1 μm scale, where smaller particles are also more abundant than the larger particles. There are few elongate-elliptical aluminosilicates ash particles (Chang et al. 1999) also in both the images which indicates that the residence time in the high-temperature zone of the furnace was too short for complete spheridization (Raask 1986). While Fig. 6c shows spherical CFA particles at 1 μm scale, where the particles are showing rectangular shaped particles, which could be depositions of aluminum in the form of mullites. While Fig. 6d also shows spherical shaped CFA particles, at 200 nm scale, where the particles are showing rectangular deposits on their surface. This indicates that the matrix has formed earlier from the molten slag and then there is the deposition of rectangular particles on their surface during cooling and condensation (Lee et al. 2002). Moreover, the external surface of most of the particles are smooth in nature.

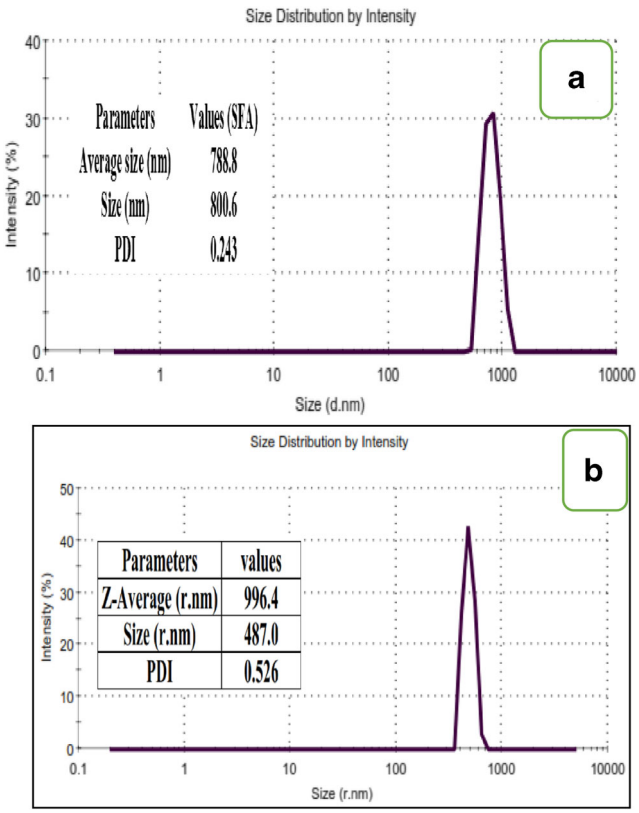

Fig. 5 Particle size distribution graph of CFA (A) and ISA (B)

Besides this, the CFA particle also has plerospheres which is not shown over here (Goodarzi and Sanei 2009). Plerospheres are particles that encapsulate numerous smaller particles within them (Sun et al. 2008). Figure 7a–d reveal the FESEM micrographs of ISA, which is clearly evident that particles are highly aggregated and present together to form lumps (Kirubakaran and Santhoshraja 2017). The ISA particles are generally irregular in shape (Fig. 7a) whose size varies from 300 nm to several microns. Some of the particles are stacked one above the other to form a cylindrical shape structure (Fig. 7d).

CFA particles also have ferrous rich spherical particles called as ferrospheres as shown in the Fig. 8a. The size of the ferrospheres from CFA over here is 4.5–6 μ and it is evident that the ferrospheres have either angular or spherules depositions on their surface. These deposited particles are ferrous which are responsible for providing magnetic properties to them. Therefore, the CFA particles have morphologically different particles like cenospheres, aluminosilicate spheres, ferrospheres, and cenospheres of variable sizes. Ferrospheres and cenospheres are more prominent in the CFA than other particles. Besides this, they also have solid spheres (precipitator), and irregular unburned carbon (Hwang et al. 2002; Dey and Pandey 2016). From the FESEM micrographs and EDS, it was revealed that the mixed ferrous-aluminosilicate content of the fly ash grains varies in intensity and texture.

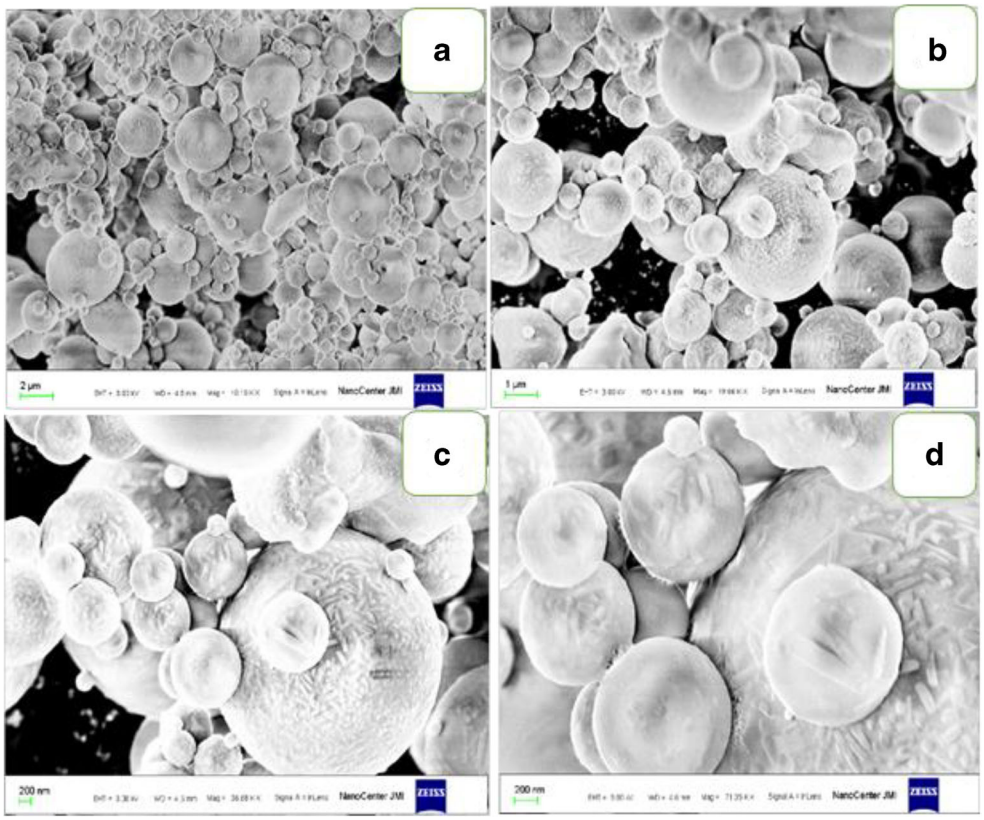

Fig. 6 FESEM micrographs of CFA particles at lower resolution (**a**–**c**), CFA particles at higher resolution along with rectangular deposits (**d**)

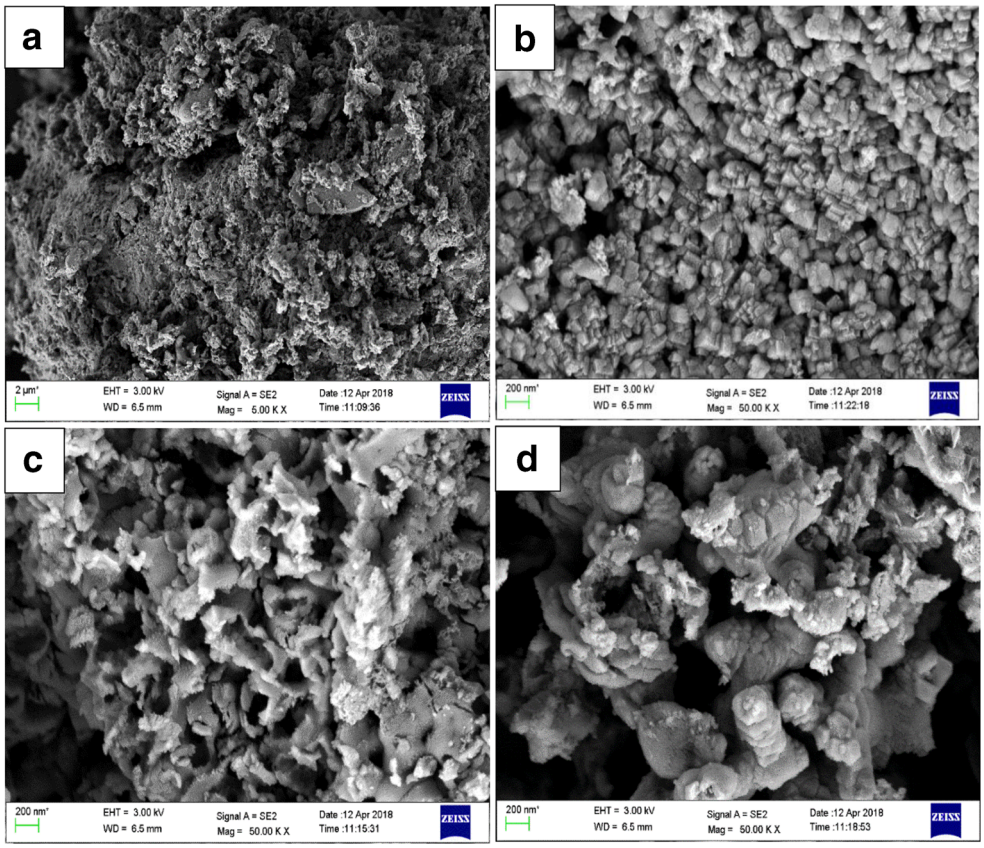

Fig. 7 FESEM micrographs of ISA at different resolution

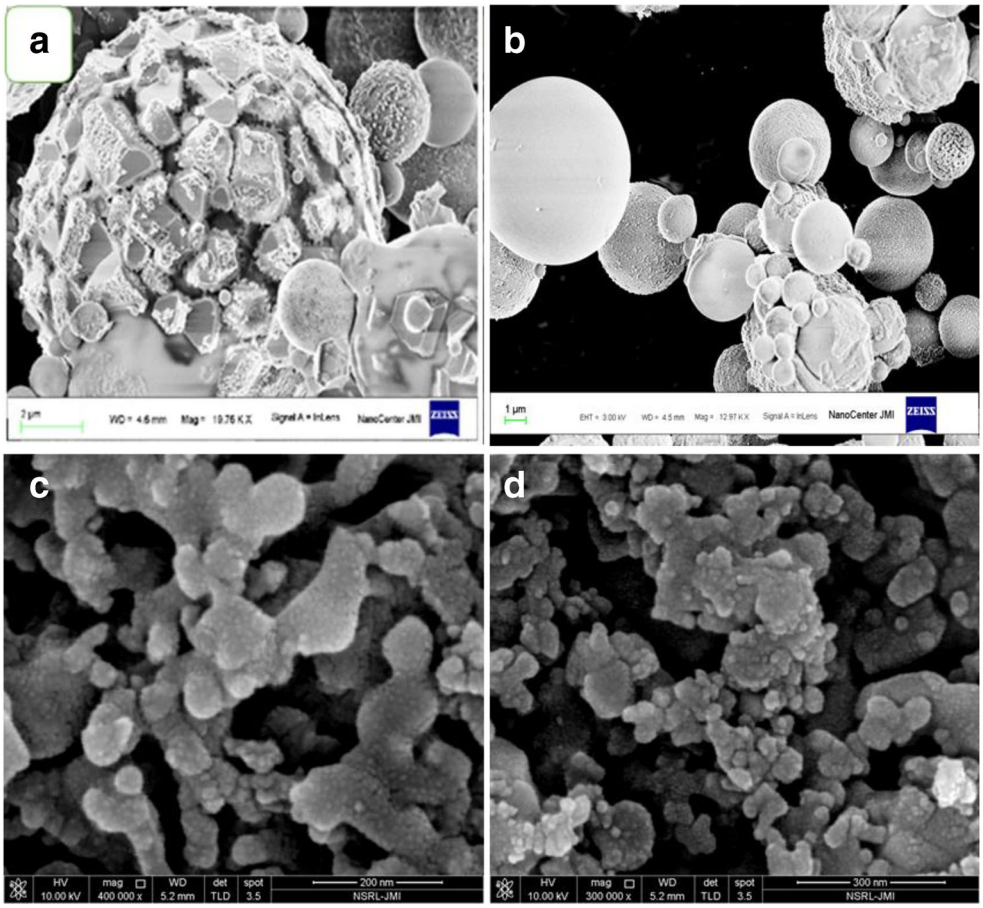

Fig. 8 FESEM of ferrous particles of CFA (**a** and **b**) and ISA (**c** and **d**)

Morphological analysis of CFA and ISA particles by FESEM showed that CFA particles are mainly spherical shaped of size 0.2 to 7 microns whereas the ISA particles were irregularly shaped whose size was varying from 300 nm to several microns. The regular spherical shape of CFA could be due to the combustion of coal matters in burner under controlled conditions which might have provided sufficient time to the molten slag to take a suitable spherical shape at high temperature. While the deposited particles are due to the depositions of particles on the preformed spherical particles in CFA.

Contrary to this, in ISA, as the temperature is not as much as that of the furnace, so the content does not reach the molten state, so the particle rearrangement in shape is not possible. Moreover, since ISA has high carbon content so the shape is also irregular in ISA particles. The unburnt incense particles had larger particle size, i.e., 1–20 microns whereas the ash of incense sticks contained particle size of about 300 nm.

In spite of non-ferrous particles there are ferrous rich particles in both the types of ashes (Table 2) which have either depositions of ferrous on a preformed cenospheres or aluminosilicate spheres surface. Secondly, spherical shaped ferrous particles, having even distribution of ferrous on their surface known as smooth ferrospheres, formed from molten slag of the coal during combustion of coal in the furnace. The ferrous particles of CFA are spherical in shape along with angular iron oxide particle depositions on their surface which is shown in Fig. 8a. CFA have ferrous particles having granular or spherule shaped iron oxide depositions on their surface. The ferrous particles of CFA are mostly spherical in shape which has either angular, granular depositions and has rough texture while few spherical particles could be smooth-surfaced (Fig. 8a, b) and due to spherical shape such particles are called ferrospheres (Vu et al. 2019; Yadav and Fulekar 2020). Their size is also similar to normal fly ash particles, i.e., in microns; while the ferrous particles of ISA are irregular shaped, small in size, highly aggregated to form a lump as shown in Fig. 8c, d. So, the ferrospheres of CFA are well organized, having a high amount of ferrous particles, and hence more magnetic in nature than the ferrous particles of ISA. But the ISA ferrous fractions have a large amount of carbon than the ferrous particles of CFA (Yadav et al. 2020a, 2020b).

TEM: morphology of CFA and ISA

The internal morphology of CFA particles is very diverse and complex (Fan et al. 2016; Thipse et al. 2002). The TEM

analysis of CFA reveals that the particles are spherical in shape with varying sizes. The size of CFA particles are 500 nm to several microns, where few particles are smaller than 200 nm while few are of 4–5 μ. Some of the CFA particles are dense black in color, spherical-shaped, rich in metallic content, i.e., Al and Fe and devoid of carbon content as in Fig. 9a. The light-dark or brighter particles are either Si-rich or carbonaceous particles (Chen et al. 2005) as shown in Fig. 9c and devoid of Fe or Al like electron rich elements. There are presences of carbonaceous particles also mainly soots, chars, and unburned carbon in the CFA, which are generally irregular in shape and brighter in color under the TEM field. The scattering area electron diffraction (SAED) pattern indicates the crystalline nature of the CFA particles as shown in Fig. 9d. The CFA fractions with larger particle size contained more unburned carbon than those with finer particle size. The unburned carbon as a porous material could have a greater surface area than the CFA particles, contributing to increase in specific surface area in CFA fractions with larger particles and more unburned carbon (Zhu et al. 2013).

In Fig. 10a, b, TEM micrographs of ISA particles reveal the larger aggregated particles of variable sizes. The scanned area was under the range of 1 micron to 50 nm which included dark color solid particles along with light aggregated clusters including irregular shape and sizes as ISA has involved different solid, semi-solids contents on it. It is predicted that the dark larger dense particles are corresponding to high weighted ferrous and electron-rich regions (Fig. 10a) while Fig. 10b shown brighter color images suggesting the lightweight carbon-rich particles along with smaller sizes as compared to ferrous rich region. So both the light and heavyweight contents of ISA particles respond differently under TEM analysis in terms of darker and brighter aggregated particles.

For the crystalline nature of the scanned particles, the scattering area electron diffraction (SAED) pattern is taken which shown a crystalline solid diffraction pattern for the involved contents like ferrous and calcium particles. The scattered diffraction pattern indicates the polycrystalline nature of the ISA particles (Fig. 10d) which have 0.26 nm d spacing (Zhang 2014) as shown in Fig. 10c. The TEM analyses of both CFA and ISA revealed that CFA particles are spherical, well organized, and electron-dense means rich in metals (Assi et al. 2020). On the other hand, ISA particles are irregular shapes and variable sizes which have dark as well as light particles which indicate the presence of a large number of carbon particles. The brighter particles are less electron-rich particles like carbon. While SAED pattern reveals that both the particles are polycrystalline in nature which was also justified by the XRD.

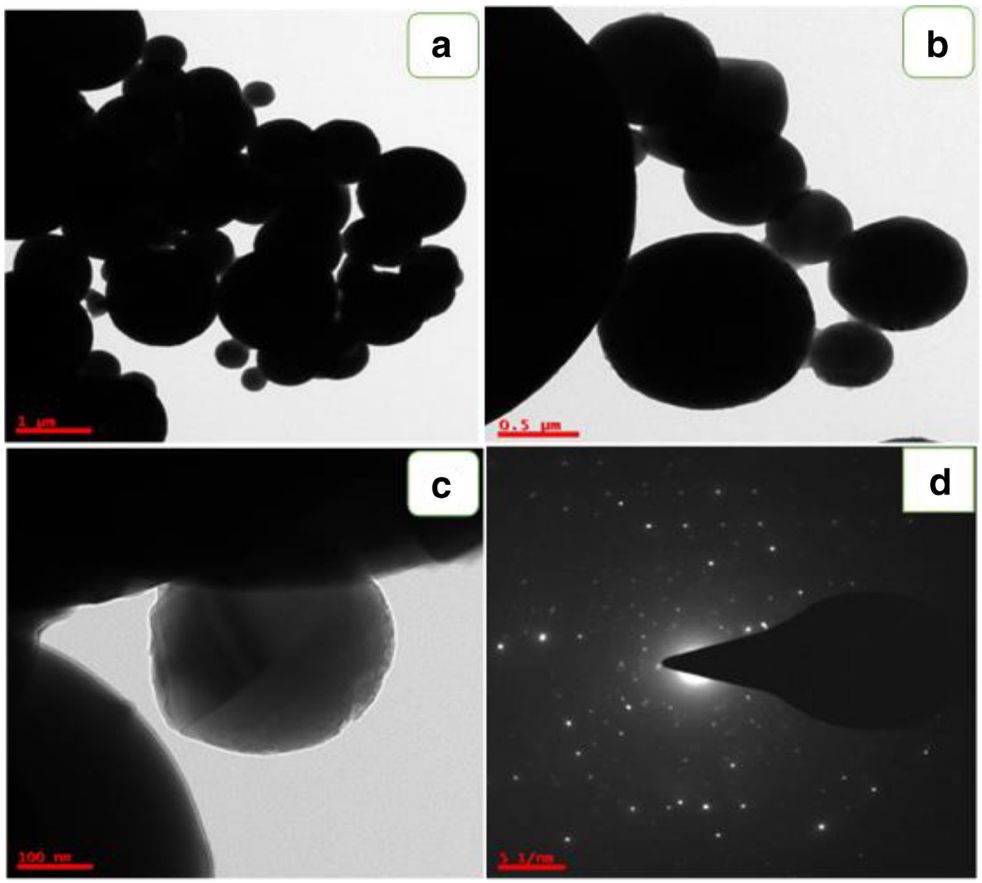

Fig. 9 TEM images of CFA (**a**–**c**) and SAED pattern (d)

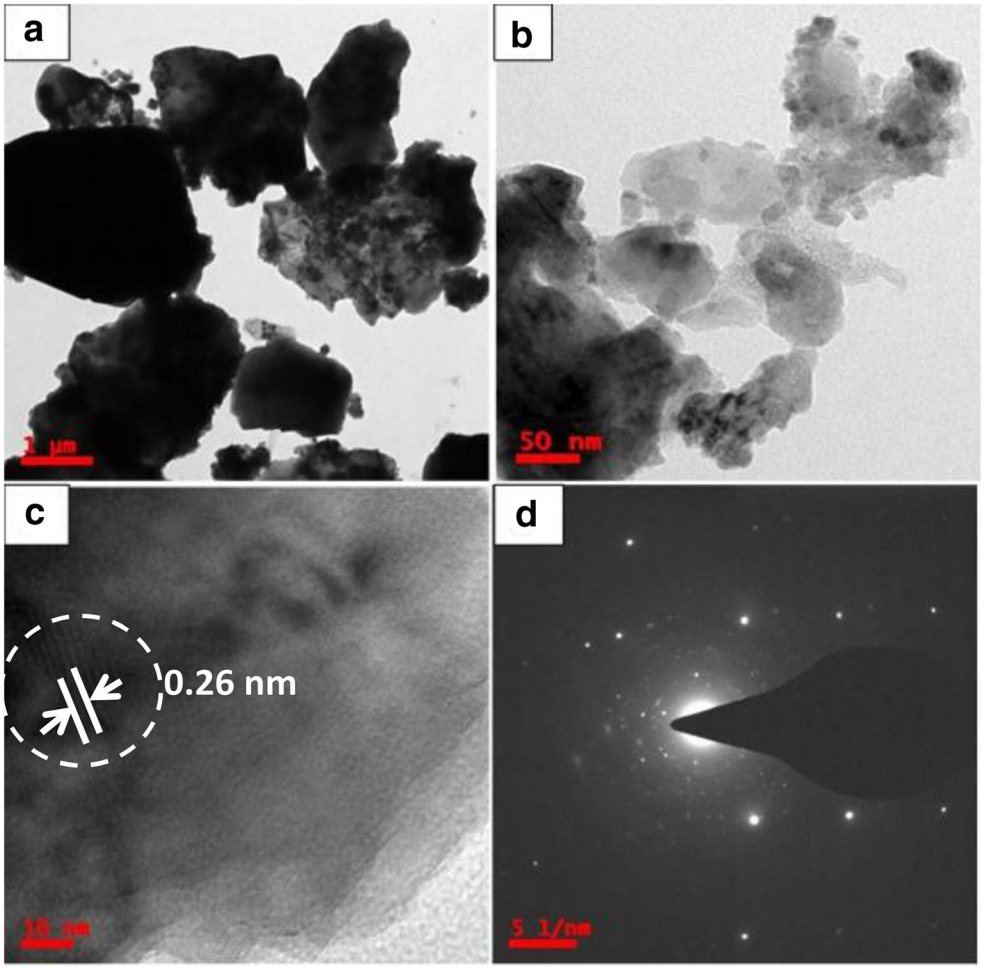

Fig. 10 TEM micrograph of **a** ferrous rich region, **b** carbon-Ca rich region, **c** HRTEM-d spacing, and **d** SAED pattern

Conclusions

The coal collected from the thermal power plant, belonged to class F, which has 87% FAS and less than 1% CaO. This clearly indicates that the thermal power plant uses better grades of coal, i.e., either bituminous or anthracite coal. The fly ash has 47% silica, 25% alumina, and 15% ferrous, which makes them suitable for the recovery of these value added minerals. Further, fly ash may also be applied in the field of zeolites and geopolymers due to their high silica to alumina ratio. In general, CFA finds applications in ceramics, civil engineering, and metallurgy. The XRF, ICP-AES and EDS revealed the presence of 46 elements in CFA. As, the CFA are derived from coal so they represents their parent molecule, i.e., coal. FTIR and XRD investigation of CFA revealed the presence of mullite, quartz, amorphous glassy silica and iron oxides as crystalline minerals. While microscopic investigation of CFA by FESEM and TEM revealed the presence of well organized, spherical shaped ferrospheres, plerospheres and cenospheres whose size was varying from 0.02 u to 7 microns.

While, on the other hand the total FAS content in ISA was 29.41% and CaO alone was 49.6%, this was due to the lesser amount of coal powder in incense sticks. While the higher amount of CaO in ISA is due to the utilization of calcium phthalate in order to minimize the smoke released from incense sticks. The XRF, ICP-AES, and EDS revealed the presence of almost similar elements as of CFA. While FTIR and XRD analysis of ISA revealed the presence of silicates, calcites, and iron oxides along with carbonates. There was absence of crystalline minerals from ISA, as in CFA. While, microscopy of ISA revealed that the well-developed, spherical structures were absent from the ISA. Instead, the ISA particles were mainly, carbon and calcium rich, irregular whose size was varying from 300 nm to several microns.

So, from the detailed instrumental analysis of CFA and ISA, it was concluded that temperature plays a major role in deciding the shape of the particles; so, CFA has obtained better shape due to combustion at higher temperatures in comparison to incense sticks. Moreover, CFA has morphologically, other spherical shaped particles like ferrospheres and cenospheres and precipitators which were missing from the ISA. Cenospheres were more prominent than the ferrospheres in the CFA particles wherein ISA irregular carbon particles were more dominant. Both have unburned carbon and soots,

due to incomplete combustion of coal or incense sticks but comparatively ISA have several folds higher amount of unburnt carbon due to bamboo sticks, fragrances, binder, and wood chips. Both the ashes have several toxic heavy metals whose direct disposal to rivers and their use as land-fills may challenge a potential threat to the living beings due to heavy metal leaching from them to nearby areas. Based on the CFA composition and comprehensive analysis, it is suitable for recovery of ferrous, silica and alumina as value added minerals. While ISA could be applied for the recovery of calcium oxides or carbonates, magnesium oxides, silica, ferrous, and carbon particles. The possible suggested applications of CFA and ISA may act as an economical and renewable source of value added minerals by minimizing the solid waste pollution from the environment.

Abbreviations *3Al2O3·2SiO2,* mullite; *Al2O3,* aluminum oxide; *CaO,* lime; *Ce,* cerium; *CFA,* coal fly ash; *CTPPs,* coal-based thermal power plants; *Dy,* dysposium; *EDS,* electron diffraction spectroscopy; *Fe2O3,* hematite, ferrous; *FESEM,* field emission scanning electron microscopy; *FTIR,* Fourier transform infrared spectroscopy; *HF,* hydrofluoric acid; *ICP-AES,* inductively coupled plasma atomic emission spectroscopy; *ISA,* incense sticks ash; *MTs,* million tons; *Na2O,* sodium dioxide; *PAH,* polyaromatic hydrocarbons; *PCHs,* polyaromatic cyclic hydrocarbons; *PDI,* poly dispersity index; *PSA,* particle size analyzer; *SAED,* scattering area electron diffraction; *Sc,* scandium; *SiO2,* quartz, silica; *TEM,* transmission electron microscopy; *Th,* thorium; *TiO2,* titanium dioxide, gypsum, and rutile; *TPPs,* thermal power plants; *XRD,* X-ray diffraction; *XRF,* X-ray fluorescence spectroscopy; *Y,* yttrium; *Yb, V, Er,* erbium

Acknowledgements The authors are also thankful to the Central Instrument Facility-Centre for Nanosciences and Nanotechnology of Jamia Millia Islamia, New Delhi, SRM–University, Chennai, CECRI (CSIR)-Karikudi, Tamil Nadu, and School of Chemistry-Hyderabad University, Telangana, for extending their instrumentation facilities.

Author contribution VKY investigated the samples for ICP-AES, XRF, and EDS, and prepared original draft of the manuscript. Material preparation, data collection, and analysis were performed by GG. MMSCP and JA investigated and interpreted XRD, FTIR, and PSA results. MA and NG critically revised the manuscript. BS analyzed and interpreted FESEM micrographs. NC analyzed and interpreted TEM micrographs. GKI prepared original draft of the manuscript. KKY supervised the prepared original draft and revised of the manuscript. All authors read and approved the final manuscript.

Funding The authors extend their sincere appreciation to researchers supporting project number (RSP-2020/129), King Saud University, Riyadh, Saudi Arabia, for funding this research.

Data availability Data sharing not applicable to this article as no datasets were generated or analyzed during the current study.

Declarations

Ethics approval and consent to participate Not applicable

Consent for publication Not applicable

Competing interests The authors declare no competing interests.

References

Abdelrazek EM, Abdelghany AM, Badr SI, Morsi MA (2018) Structural, optical, morphological and thermal properties of PEO/PVP blend containing different concentrations of biosynthesized Au nanoparticles. J Mater Res Technol 7:419–431

Ahmari S, Zhang L (2015) The properties and durability of alkali-activated masonry units. In: Pacheco-Torgal F, Labrincha JA, Leonelli C, Palomo A (eds) Handbook of alkali-activated cements, mortars and concretes. Woodhead Publishing, pp 643-660.

Aich S, Nandi BK, Bhattacharya S (2019) Effect of weathering on physico-chemical properties and combustion behavior of an Indian thermal coal. Int J Coal Sci Technol 6:51–62

Alam J, Yadav VK, Yadav KK, Cabral-Pinto MMS, Tavker N, Choudhary N, Shukla AK, Ali FAA, Alhoshan M, Alehyen S, Achouri ME, Taibi M (2017) Characterization, microstructure and properties of fly ash-based geopolymer. J Mater Environ Sci 8: 1783–1796

Alehyen S, Achouri ME, Taibi M (2017) Characterization, microstructure and properties of fly ash-based geopolymer. J Mater Environ Sci 8(5):1783–1796

Assi A, Bilo F, Zanoletti A, Ponti J, Valsesia A, Spina LR, Bontempi E (2020) Review of the reuse possibilities concerning ash residues from thermal process in a medium-sized urban system in Northern Italy. Sustainability 12:4193

Aughenbaugh KL, Stutzman P, Juenger MCG (2016) Identifying glass compositions in fly ash. Front Mater. https://doi.org/10.3389/fmats.2016.00001

Ayanda OS, Fatoki OS, Adekola FA, Ximba BJ (2012) Characterization of fly ash generated from Matla power station in Mpumalanga, South Africa. E-J Chem 9(4):1788–1795

Bacsik Z, Mink J, Keresztury J (2004) FTIR spectroscopy of the atmosphere. I. principles and methods. Appl Spectrosc Rev 39:295–363

Bartoňová L (2015) Unburned carbon from coal combustion ash: an overview. Fuel Process Technol 134:136–158

Benarchid MY, Rogez J, Diouri A, Boukhari A, Aride J (2005) Formation and hydraulic behavior of chromium-phosphorus doped calcium sulfoaluminate cement. Thermochim Acta 433:183–186

Cabral-Pinto MMS, Ferreira da Silva EA, MMVG S, Melo-Gonçalves P, Candeias C (2014) Environmental risk assessment based on high-resolution spatial maps of potentially toxic elements sampled on stream sediments of Santiago, Cape Verde. Geosciences 4:297–315

Cabral-Pinto MMS, Inácio M, Neves O, Almeida AA, Pinto E, Oliveiros B, Ferreira da Silva EA (2020) Human health risk assessment due to agricultural activities and crop consumption in the surroundings of an industrial area. Exposure and Health 12:629–640

Cabral-Pinto MMS, Ferreira da Silva EA (2019) Heavy metals of Santiago island (Cape Verde) alluvial deposits: Baseline value maps and human health risk assessment. Int J Environ Res Public Health 16(1):2

CEA (2019) Annual report 2017-18. Central Electricity Authority, Government of India, Ministry of Power

Chang H-L, Chun CM, Aksay IA, Shih W-H (1999) Conversion of fly ash into mesoporous aluminosilicate. Ind Eng Chem Res 38(3):973–977

Chen Y, Shah N, Huggins FE, Huffman GP (2005) Transmission electron microscopy investigation of ultrafine coal fly ash particles. Environ Sci Technol 39:1144–1151

Choo TF, Salleh MAM, Kok KY, Matori KA, Rashid SA (2020) Effect of temperature on morphology, phase transformations and thermal expansions of coal fly ash cenospheres. Crystals 10:481

Choudhary N, Yadav VK, Malik P, Khan SH, Inwati GK, Suriyaprabha R, Singh B, Yadav AK, Ravi RK (2020) Recovery of natural nanostructured minerals: Ferrospheres, plerospheres, cenospheres, and carbonaceous particles from fly ash. In: Duca G, Vaseashta A (eds) Handbook of research on emerging developments and environmental impacts of ecological chemistry. IGI Global, pp 450-470.

Dewangan S, Chakrabarty R, Zielinska B, Pervez S (2013) Emission of volatile organic compounds from religious and ritual activities in India. Environ Monit Assess 185:9279–9286

Dey A, Pandey KM (2016) Characterization of fly ash and its reinforcement effect on metal matrix composites: A review. Rev Adv Mater Sci 44:168–181

Fan J, Shao L, Hu Y, Wang J, Wang J, Ma J (2016) Classification and chemical compositions of individual particles at an eastern marginal site of Tibetan Plateau. Atmos Pollut Res 7:833–842

Fernández-Jiménez A, Palomo A (2005) Mid-infrared spectroscopic studies of alkali-activated fly ash structure. Microporous Mesoporous Mater 86:207–214

Fernández-Jiménez A, García-Lodeiro I, Donatello S, Maltseva O, Palomo Á (2014) Specific examples of hybrid alkaline cement. MATEC Web of Conferences 11:01001

Fuller A, Maier J, Karampinis E, Kalivodova J, Grammelis P, Kakaras E, Scheffknecht G (2018) Fly ash formation and characteristics from (co-)combustion of an herbaceous biomass and a Greek lignite (low-rank coal) in a pulverized fuel pilot-scale test facility. Energies 11: 1581

Gerardo B, Cabral Pinto M, Nogueira J, Pinto P, Almeida A, Pinto E, Marinho-Reis A, Diniz L, Moreira PI, Simões MR, Freitas S (2020) Associations between trace elements and cognitive decline: an exploratory 5-year follow-up study of an elderly Cohort. Int J Environ Res Public Health 17:6051

Gomes S, François S (2000) Characterization of mullite in silicoaluminous fly ash by XRD, TEM, and ^{29}Si MAS NMR. Cem Concr Res 30:175–181

Goodarzi F, Sanei H (2009) Plerosphere and its role in reduction of emitted fine fly ash particles from pulverized coal-fired power plants. Fuel 88:382–386

Gupta N, Yadav KK, Kumar V (2015) A review on current status of municipal solid waste management in India. J Environ Sci 37: 206–217

Gupta N, Yadav KK, Kumar V, Krishnan S, Kumar S, Nejad ZD, Khan MAM, Alam J (2021) Evaluating heavy metals contamination in soil and vegetables in the region of North India: Levels, transfer and potential human health risk analysis. Environ Toxicol Pharmacol 82:103563

Hariharan M, Varghese N, Cherian AB, Sreenivasan PV, Paul J, Antony AKA (2014) Synthesis and characterisation of $CaCO_3$ (calcite) nano particles from cockle shells using chitosan as precursor. International Journal of Scientific 4:1–5

Haustein E, Kuryłowicz-Cudowska A (2020) The effect of fly ash microspheres on the pore structure of concrete. Minerals 10:58

Hwang JY, Sun X, Li Z (2002) Unburned carbon from fly ash for mercury adsorption: I Separation and characterization of unburned carbon. J Miner Mater Charact Eng 1:39–60

Jaarsveld JGSV, Deventer JSJV, Lukey GC (2003) The characterisation of source materials in fly ash-based geopolymers. Mater Lett 57: 1272–1280

Jeyageetha CJ, Kumar SP (2013) Study of SEM/EDXS and FTIR for fly ash to determine the chemical changes of ash in marine environment. Int J Sci Res 5:1688–1693

Jóźwiak-Niedźwiedzka D, Glinicki MA, Gibas K, Baran T (2018) Alkali-silica reactivity of high density aggregates for radiation shielding concrete. Materials (Basel) 11:2284

Kanchan S, Kumar V, Yadav KK, Gupta N, Arya S, Sharma S (2015) Effect of fly ash disposal on ground water quality near Parichha thermal power plant, Jhansi: a case study. Curr World Environ 10: 572–580

Khale D, Chaudhary R (2007) Mechanism of geopolymerization and factors influencing its development: a review. J Mater Sci 42:729–746

Khatri C, Rani A (2008) Synthesis of a nano-crystalline solid acid catalyst from fly ash and its catalytic performance. Fuel 87:2886–2892

Kirubakaran D, Santhoshraja V (2017) Utilization of Pelletized fly ash aggregate to replace the natural aggregate: A Review. Int Res J Eng Technol 4:148–151

Lee WKW, Deventer V (2002) Structural reorganisation of class F fly ash in alkaline silicate solutions. Colloids Surf A Physicochem Eng Aspects 211:49–66

Lee BE, Fletcher CAJ, Shin SH, Kwon SB (2002) Computational study of fouling deposit due to surface-coated particles in coal-fired power utility boilers. Fuel 81:2001–2008

Leelarungroj K, Likitlersuang S, Chompoorat T, Janjaroen D (2018) Leaching mechanisms of heavy metals from fly ash stabilised soils. Waste Manag Res 36:616–623

Li LS, Wu YS, Liu YY, Zhai YC (2011) Extraction of alumina from coal fly ash with sulfuric acid leaching method. Chin J Process Eng 11(2):254–258

Liao F, Guo X-M (2019) The effects of Al_2O_3 and SiO_2 on the formation process of silico-ferrite of calcium and aluminum (SFCA) by solid-state reactions. Minerals 9:101

Lin T-C, Krishnaswamy G, Chi DS (2008) Incense smoke: clinical, structural and molecular effects on airway disease. Clin Mol Allergy 6:3

Liu J, Zhang F, Hou L, Li S, Gao Y, Xin Z, Li Q, Xie S, Wang N, Zhao Y (2020) Synergistic engineering of 1D electrospun nanofibers and 2D nanosheets for sustainable applications. Sustain Mater Technol 26: e00214

Makaka G (2014) Influence of fly ash on brick properties and the impact of fly ash brick walls on the indoor thermal comfort for passive solar energy efficient house. Comput Water Energy Environ Eng 3:152–161

Malav LC, Yadav KK, Gupta N, Kumar S, Sharma GK, Krishnan S, Rezania S, Kamyab H, Pham QB, Yadav S, Bhattacharyya S, Yadav VK, Bach Q-V (2020) A review on municipal solid waste as a renewable source for waste-to-energy project in India: current practices, challenges, and future opportunities. J Clean Prod 277: 123227

Manocha LM, Ram KA, Manocha SM (2011) Separation of cenospheres from fly ashes by floatation method. Eurasian Chem Tech J 13:89–95

Marjanović A, Vujnović S, Đurović Ž (2020) One approach to temperature distribution control in thermal power plant boilers. Automatika 61:273–283

Menazea AA (2020) One-pot pulsed laser ablation route assisted copper oxide nanoparticles doped in PEO/PVP blend for the electrical conductivity enhancement. J Mater Res Technol 9:2412–2422

Miricioiu MG, Niculescu V-C (2020) Fly Ash, from recycling to potential raw material for mesoporous silica synthesis. Nanomaterials 10:474

Misra NL, Mudher KDS (2002) Total reflection X-ray fluorescence: a technique for trace element analysis in materials. Prog Cryst Growth Charact Mater 45:65–74

Mollah MYA, Promreuk S, Schennach R, Cocke DL, Güler R (1999) Cristobalite formation from thermal treatment of Texas lignite fly ash. Fuel 78:1277–1282

Ogunsona EO, Grovu T, Mekonnen TH (2020) Fabrication of nanostructured graphene oxide-like few-layer sheets from biocarbon via a green process. Sustain Mater Technol 26:e00208

Ohenoja K, Pesonen J, Yliniemi J, Illikainen M (2020) Utilization of fly ashes from fluidized bed combustion: A review. Sustainability 12: 2988

Pal MK, Gautam J (2012) Synthesis and characterization of polyacrylamide-calcium carbonate and polyacrylamide-calcium sulfate nanocomposites. Polym Compos 33(4):515–523

Palomo A, Krivenko P, Garcia-Lodeiro I, Kavalerova E, Maltseva O, Fernández-Jiménez A (2014) A review on alkaline activation: new analytical perspectives. Mater Constr 64:e022

Prasad B, Mondal KK (2008) Heavy metals leaching in Indian fly ash. J Environ Sci Eng 50(2):127–132

Prochon P, Zhao Z, Courard L, Piotrowski T, Michel F, Garbacz A (2020) Influence of activators on mechanical properties of modified fly ash based geopolymer mortars. Materials 13(5):1033

Qin Z, Song Y, Jin Y (2019) Green worship: the effects of devotional and behavioral factors on adopting electronic incense products in religious practices. Int J Environ Res Public Health 16:3618

Raask E (1986) Flame vitrification and sintering characteristics of silicate ash. In: Vorres KS (ed) Mineral matter and ash in coal. ACS symposium series, Washington, American Chemical Society, pp 115–138.

Ramya HG, Palanimuthu V, Kumar R (2013) Patchouli in fragrances-incense stick production from patchouli spent charge powder. Agric Eng Int CIGR J 15:187–193

Ranjbar N, Kuenzel C (2017) Cenospheres: A review. Fuel 207:1–12

Reig FB, Adelantado JVG, Moreno MCMM (2002) FTIR quantitative analysis of calcium carbonate (calcite) and silica (quartz) mixtures using the constant ratio method. Application to geological samples. Talanta 58:811–821

Rosas-Casarez CA, Arredondo-Rea SP, Cruz-Enríquez A, Corral-Higuera R, Pellegrini-Cervantes MDJ, Gómez-Soberón JM, Medina-Serna TDJ (2018) Influence of size reduction of fly ash particles by grinding on the chemical properties of geopolymers. Appl Sci 8:365

Salah N, Habib S, Khan ZH, Alshahrie A, Memic A, Al-ghamdi AA (2016) Carbon rich fly ash and their nanostructures. Carbon Lett 19:23–31

Satapathy A, Prasad S, Mishra D (2010) Development of protective coatings using fly ash premixed with metal powder on aluminium substrates. Waste Manag Res 28(7):660–666

Sear LKA (2001) The properties and use of coal fly ash. Thomas Telford Ltd., London

Shakkthivel P, Ramesh D, Sathiyamoorthi R, Vasudevan T (2005) Water soluble copolymers for calcium carbonate and calcium sulphate scale control in cooling water systems. J Appl Polym Sci 96: 1451–1459

Shan D, Zhu M, Han E, Xue X, Cosnier S (2007) Calcium carbonate nanoparticles: a host matrix for the construction of highly sensitive amperometric phenol biosensor. Biosens Bioelectron 23:648–654

Sharma S, Kumar V, Yadav KK, Gupta N, Verma C (2015) Long-term assessment of fly ash disposal on physico-chemical properties of soil. Int J Curr Res Biosci Plant Biol 2:105–110

Sharma S, Kumar V, Yadav KK, Gupta N, Vishwakarma SK (2016) Effect of fly ash deposition on biochemical parameters of different crop plants around Parichcha thermal power plant, Jhansi, India. Int J Curr Microbiol App Sci 5:873–877

Shi-Chih C, Hsiang-Sheng K (1993) A study of engineering properties of a clay modified by fly ash and slag. Fly ash for soil improvement. Asce geotechnical special publication no 36, American Society of Civil Engineers 345 East 47th Street New York, NY United States pp 89-99.

Shoumkova AS (2010) Magnetic separation of coal fly ash from Bulgarian power plants. Waste Manag Res 29:1078–1089

Sun JM, Yao Q, Xu X-C (2008) Classification of micro-particles in fly ash. Dev Chem Eng Miner Process 9:233–238

Suriyanarayanan N, Nithin KVK, Bernardo E (2009) Mullite glass ceramics production from coal ash and alumina by high temperature plasma. J Non-Oxide Glasses 1:247–260

Tavker N, Yadav VK, Yadav KK, Cabral-Pinto MM, Alam J, Shukla AK, Ali FAA, Alhoshan M (2021) Removal of cadmium and chromium by mixture of silver nanoparticles and nano-fibrillated cellulose isolated from waste peels of citrus sinensis. Polymers 13:234

Thipse SS, Schoenitz M, Dreizin EL (2002) Morphology and composition of the fly ash particles produced in incineration of municipal solid waste. Fuel Process Technol 75:173–184

Valeev D, Mikhailova A, Atmadzhidi A (2018) Kinetics of iron extraction from coal fly ash by hydrochloric acid leaching. Metals 8:533

Verma R, Patel KS, Verma SK (2014) Chemical composition of indoor ash residues. J Adv Environ Health Res 2:81–90

Vu D-H, Bui H-B, Kalantar B, Bui X-N, Nguyen D-A, Le Q-T, Nguyen H (2019) Composition and morphology characteristics of magnetic fractions of coal fly ash Wastes processed in high-temperature exposure in thermal power plants. Appl Sci 9:1964

Wang S, Soudi M, Li L, Zhu ZH (2006) Coal ash conversion into effective adsorbents for removal of heavy metals and dyes from wastewater. J Hazard Mater B133:243–251

Ward CR (2002) Analysis and significance of mineral matter in coal seams. Int J Coal Geol 50:135–168

Wilińska I, Pacewska B (2019) Comparative investigation of reactivity of different kinds of fly ash in alkaline media. J Therm Anal Calorim 138:3857–3872

Wrona J, Żukowski W, Bradło D, Czupryński P (2020) Recovery of cenospheres and fine fraction from coal fly ash by a novel dry separation method. Energies 13:3576

Yadav VK, Fulekar MH (2020) Advances in methods for recovery of ferrous, alumina, and silica nanoparticles from fly ash waste. *Ceramics 3*:384–420

Yadav VK, Pandita PR (2019) Fly ash properties and their applications as a soil ameliorant. In: Rathoure AK (ed) Amelioration technology for soil sustainability. IGI Global pp 59-89.

Yadav VK, Singh B, Choudhary N (2020a) Characterization of Indian incense stick powders for their physical, chemical and mineralogical properties. World J Environ Biosci 9:39–43

Yadav VK, Yadav KK, Gnanamoorthy G, Choudhary N, Khan SH, Kamyab H, Bach Q-V (2020b) Green synthesis and characterization of polyhedral shaped amorphous iron oxide nanoparticles from incense sticks ash waste. Environ Technol Innov 20:101089

Yadav VK, Kumar P, Kalasariya H, Choudhary N, Singh B, Gnanamoorthy G, Gupta N, Khan SH, Khayal A (2020c) The current scenario of Indian incense sticks market and their impact on the Indian economy. *Ind J Pure Appl Biosci 8*:627–636

Yang C-R, Lin T-C, Chang F-H (2006) Correlation between calcium carbonate content and emission characteristics of incense. J Air Waste Manage Assoc 56:1726–1732

Zhang W (2014) Nanoparticle aggregation: Principles and modeling. In: Capco D, Chen Y (eds) Advances in experimental medicine and biology. Springer, Dordrecht, pp 19–43

Zhu Z, Wang X, Dai S, Huang B, ASCE M, He Q (2013) Fractional characteristics of coal fly ash for beneficial use. J Mater Civ Eng 25:63–69

Zhuang XY, Chen L, Komarneni S, Zhou CH, Tong DS, Yang HM, Yu WH, Wang H (2016) Fly ash-based geopolymer: clean production, properties and applications. J Clean Prod 125:253–267